

Thermal radiation effect on MHD non Darcian boundary layer flow and heat transfer past an exponentially vertically stretching sheet

Ambuja Joshi

Department of Mathematics, Shankar Narayan College of Arts and Commerce, Bhayandar West Thane Maharashtra India

Abstract

The present work considers the effect of thermal radiation on MHD Non-Darcian boundary layer flow and heat transfer past an exponentially, vertically stretching sheet. The effects of various physical parameters, such as, Magnetic field parameter $\frac{Ha^2}{Re}$ Thermal buoyancy parameter Gr, Prandtl number Pr, heat source/sink parameter λ , on flow and heat transfer characteristics, are computed and represented graphically.

Key Words: Exponentially vertically stretching sheet; heat source/sink parameter; Runge-Kutta shooting method; Prandtl Number; Magnetic Field Parameter.

1. Introduction

In industrial manufacturing process the heat and mass transfer problems are well used. This phenomena applicable in wire and fibre coatings and transpiration cooling etc. In astrophysics and geophysics the MHD flow basically used. Basically the MHD flow has wide applications. Usually used in Engineering and industrial. The fluid subjected to a magnetic field become a good agreement results. There is a wide application in Mechanical Engineering field..

Stokes [1] and Gadel-Hak [2] theory. However, there are situations wherein this condition does not hold. Partial velocity slip may occur on the stretching boundary when the fluid is particulate such as emulsions, suspensions, foams and polymer solutions. Navier [3] proposed a slip boundary condition wherein the slip depends linearly on the shear stress. However, experiments suggest that the slip velocity also depends on the normal stress. H. I. Anderson [4] considered the slip flow of a Newtonian viscous fluid past a linearly stretching sheet. T. Hayat, T. Javed, Z. Abbas [5] studied M.H.D steady flow of second grade fluid with transfer analysis. The flow in a porous space is due to a stretching sheet which also exhibits slip condition. Bikash Sahoo [6] studied the effect of partial slip on the steady flow and heat transfer of an incompressible, thermo-dynamically compatible third grade fluid past a stretching sheet.

A number of models have been advanced for describing the slip that occurs at solid boundaries. A brief description of these models can be found in the work of Rao and Rajagopal [7]. Elbashbeshy [8] has added a new dimension in his investigation by considering the flow and heat transfer of a Newtonian fluid over

an exponentially stretching continuous surface. He considered an exponential stretching velocity distribution on the coordinate considered in the direction of stretching. P. Donald Ariel [9] studied the steady, laminar, axisymmetric flow of an incompressible viscous Newtonian fluid past a stretching sheet when there is a partial slip at the boundary. Bikash Sahoo, Younghae Do [10] investigated the combined effects of the non-Newtonian flow parameters, magnetic field and the partial slip on the flow and heat transfer of an electrically conducting third grade fluid arising due to the linearly stretching sheet. Present work discusses MHD thermal radiation effect over an exponentially vertically stretching sheet

The effect of various physical parameters are also discussed in detail.

2. Diagram Specifying Flow Creation

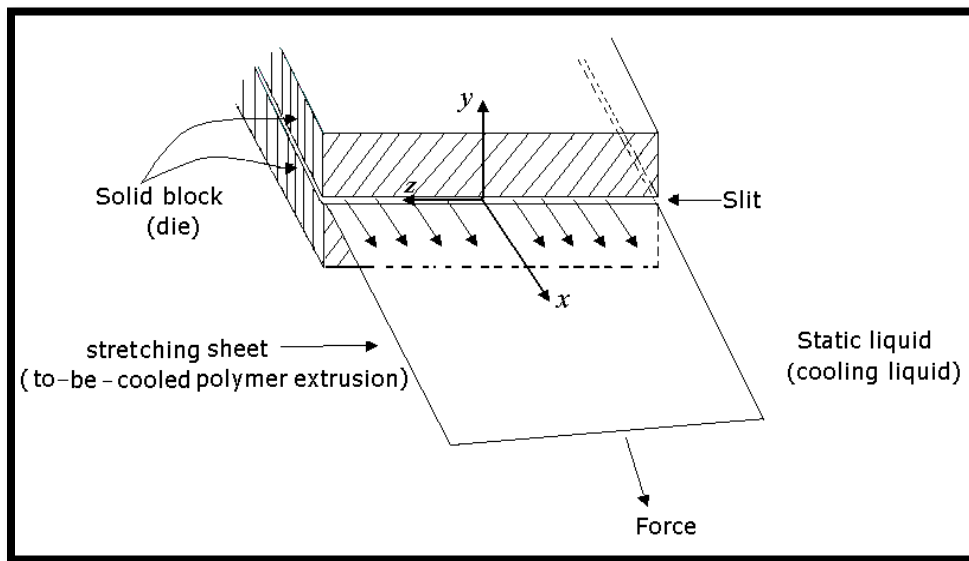


Fig. 1: Schematic of the stretching sheet problem

3. Flow analysis

The sheet lies in the plane $y = 0$ with the flow being confined to $y > 0$. Two equal and opposite forces are applied along the x -axis, so that the sheet is stretched, keeping the origin fixed. Under the boundary layer approximation and the assumption that the contribution due to the normal stress is of the same order of magnitude as the shear stress, the basic boundary layer equations governing equations are given by,

$$\frac{\partial u}{\partial x} + \frac{\partial v}{\partial y} = 0, \quad (3.1)$$

$$u \frac{\partial u}{\partial x} + v \frac{\partial u}{\partial y} = \nu \frac{\partial^2 u}{\partial y^2} - \frac{\nu}{k} u - \frac{C_b}{\sqrt{k}} u^2 + g\beta(T - T_\infty) - \sigma \frac{B_0^2}{\rho} u \quad (3.2)$$

$$u \frac{\partial T}{\partial x} + v \frac{\partial T}{\partial y} = \alpha \frac{\partial^2 T}{\partial y^2} + \frac{\sigma}{\rho C_p} B_0^2 u^2 + \frac{\mu}{\rho C_p} \left(\frac{\partial T}{\partial y} \right)^2 + \frac{Q}{\rho C_p} (T - T_\infty) - \frac{1}{\rho c_p} \frac{\partial q_r}{\partial y}, \quad (3.3)$$

The associated boundary conditions to the problem are

$$\begin{aligned} U &= U_w(x), v = 0, T = T_w(x), \text{ at } y = 0, \\ u &= 0, T \rightarrow T_\infty, \text{ as } y \rightarrow \infty \end{aligned} \quad (3.4)$$

Where u and v are the x and y components of the velocity field of the steady plane boundary flow, respectively. ν denotes the kinematic viscosity and α is the thermal diffusivity of the ambient fluid. Both are assumed to be constant, σ is the electrical conductivity and B_0 is the magnetic field flux density. The fluid flow is independent of the temperature field, T_∞ is the temperature of the ambient fluid and Q is internal heat generation/absorption coefficient. C_b is the drag coefficient. The stretching velocity U_w and exponential temperature distribution T_w are defined as

$$U_w(x) = U_0 e^{\frac{x}{L}}, \quad (3.5)$$

$$T_w(x) = T_\infty + (T_0 - T_\infty) e^{\frac{ax}{2L}},$$

Where T_0 and a are parameters of temperature distribution over the stretching surface.

T is the temperature, K is the thermal conductivity, C_p is the Specific heat and q_r is the radiative heat flux.

$$q_r = -\frac{4\sigma^* \partial T^4}{3K^* \partial y}, \quad (3.6)$$

Where K^* is the mean absorption coefficient and σ^* is the Stefan-Boltzmann Constant. T^4 is expressed as a linear function of temperature, hence

$$T^4 = 4T_\infty^3 T - 3T_\infty^4 \quad (3.7)$$

Introducing the following non-dimensional parameter :

$$\eta = \sqrt{\frac{\text{Re } y}{2L}} e^{\frac{x}{2L}}, \psi(x, \eta) = \sqrt{2 \text{Re } y} e^{\frac{x}{2L}} f(\eta), \quad (3.8)$$

$$T(x, y) = T_\infty + (T_0 - T_\infty) e^{\frac{ax}{2L}} \theta(\eta), \quad (3.9)$$

Where ψ is the stream function which is defined in the usual form as

$$u = \frac{\partial \psi}{\partial y} \text{ and } v = -\frac{\partial \psi}{\partial x} \quad (3.10)$$

Thus substituting (3.8) and (3.9) into Eq(3.10),we obtain u and v as follows:

$$u(x, y) = u_0 e^{\frac{x}{L}} f'(\eta), \quad v(x, y) = -\frac{v}{L} \sqrt{\frac{\text{Re}}{2}} e^{\frac{x}{2L}} [f(\eta) + \eta f'(\eta)]. \quad (3.11)$$

Eqns (3.1) to(3.4) is transformed into the ordinary differential equations with the aid of equations(3.8)-(3.11).Thus, the governing equations takes the form,

$$f''' + ff'' - (2 + N_2)f'^2 + 2Gre^{\frac{ax}{2}} e^{-2x}\theta - 2e^{-x}f' \left(\frac{Ha^2}{\text{Re}} + N_1\right) = 0 \quad (3.12)$$

$$\text{Pr}^{-1} \theta'' \left(1 + \frac{4K}{3}\right) + f\theta' - af'\theta + e^{\frac{X(2-a)}{2}} Ec \left(2 \frac{Ha^2}{\text{Re}} f'^2 + f'^2 e^X\right) + 2\lambda e^{-X} \theta = 0 \quad (3.13)$$

The boundary conditions (3.5) reduces to,

$$C_f \sqrt{\text{Re}_x} = \sqrt{2X} f''(0), f(0)=0, f'(0) = 1, \theta(0) = 1, \quad (3.14)$$

$$f'(\infty) = 0, \theta(\infty) = 0, \quad (3.15)$$

Where, $X = \frac{x}{L} Ha = \left(\frac{\sigma B_0^2 L^2}{\rho \nu}\right)^{\frac{1}{2}}$ is Hartman number, $Ec = U_0^2 / c_p (T_0 - T_\infty)$ is Eckert number,

$\lambda = QL^2 / (\mu c_p \text{Re})$ is the dimensionless heat generation/absorption

parameter, $Gr_1 = g\beta(T_0 - T_\infty) \frac{L^3}{\nu^2}$ is the Grashof number, $\text{Re} = U_0 L / \nu$ is Reynolds number,

$\text{Gr} = Gr_1 / \text{Re}^2$ is the thermal buoyancy parameter, and $\text{Pr} = \frac{\nu}{\alpha}$ is the Prandtl number, Where

$N_1 = \frac{L^2}{k \text{Re}}$, is the porous parameter $N_2 = 2 \frac{C_b L}{\sqrt{k}}$ is the inertia coefficient .

$\lambda = L, Z = Ha^2 / \text{Re}, a = W \cdot K = \frac{4\sigma^* T_\infty^3}{K^* K}$ Radiation Parameter. In the above system of local

similarity equations, the effect of the magnetic field is included as a ratio of the Hartman number to the Reynolds number.

The physical quantities of interest in the problem are the local skin friction acting on the surface in contact with the ambient fluid of constant density which is defined as

$$\tau_{wx} = \rho \nu \left(\frac{\partial u}{\partial y}\right)_{y=0} = \left(\frac{\rho \nu U_0}{L}\right) \left(\frac{\text{Re}}{2}\right)^{\frac{1}{2}} e^{\frac{x}{2L}} f''(0) \quad (3.16)$$

And the non-dimensional skin friction coefficient, C_f , which can be written as,

$$C_f = \frac{2\tau_{wx}}{(\rho U_w^2)} \text{ or } C_f \sqrt{\text{Re}_x} = \sqrt{2X} f''(0). \quad (3.17)$$

The local surface heat flux through the wall with k as thermal conductivity of the fluid is given by

$$q_{wx} = -k \left(\frac{\partial T}{\partial y} \right)_{y=0} = \frac{k(T_0 - T_\infty)}{L} \left(\frac{\text{Re}}{2} \right)^{\frac{1}{2}} e^{\frac{(a+1)}{2}} \theta'(0). \quad (3.18)$$

The local Nusselt number, Nu_x , which is defined as

$$Nu_x = \frac{xq_{wx}(x)}{k(T_w - T_\infty)}, \quad (3.19)$$

$$Nu_x / \sqrt{\text{Re}_x} = -(X/2)^{\frac{1}{2}} \theta'(0), \quad (3.20)$$

Where Re_x is the local Reynolds number based on the surface velocity and is given by

$$\text{Re}_x = \frac{xU_w(x)}{\nu}. \quad (3.21)$$

4. Numerical Solution

The above set Non linear differential equations(3.12)-(3.13) subject to the boundary conditions (3.14) – (3.15) are solved using Runge-Kutta Shooting Method.

3.4. Results and Discussions

Fig.2:Represents the effect of magnetic field parameter $\frac{Ha^2}{\text{Re}}$, on velocity profile f' . Here magnetic field produces a drag in the form of Lorentz force. Due to this effect, the magnitude of velocity decreases and the thermal boundary layer thickness increases.

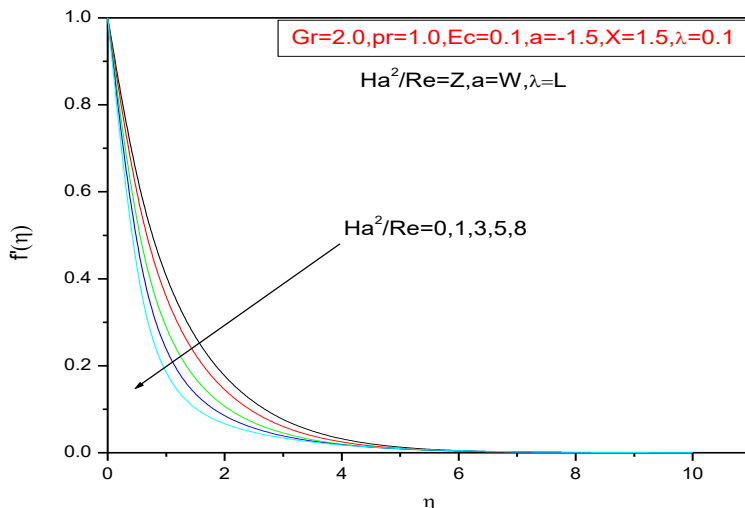


Fig 2 Effect of magnetic field on velocity profiles with η

Fig.3: Represents the various values of parameter a with velocity profile. From this figure, it is observed that the value of a increases with increase in the velocity flow. and maximum velocity occurs at $a=7$.

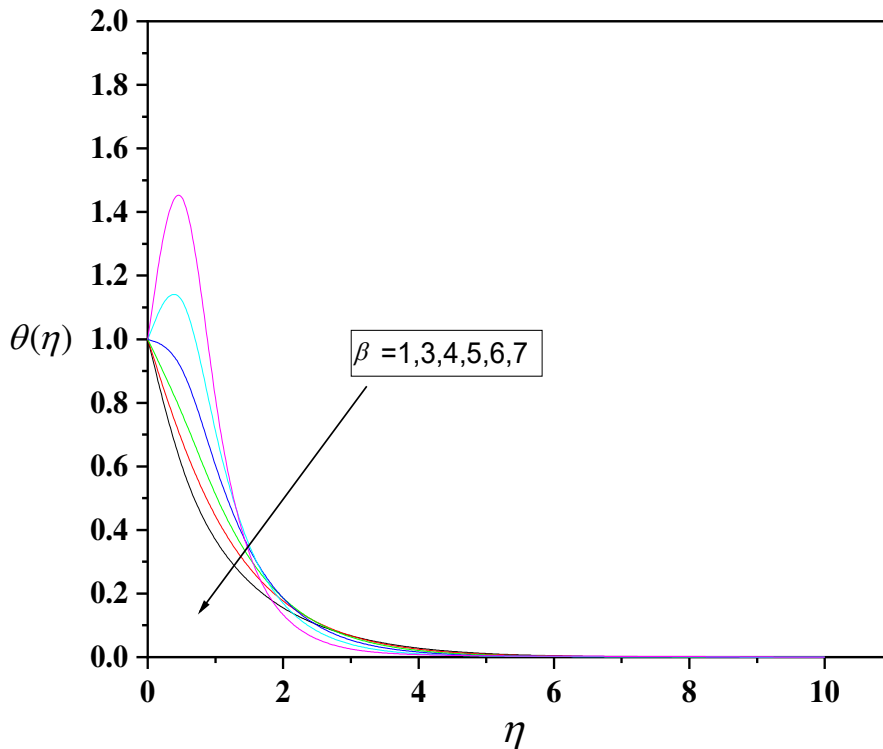


Fig.3. Variation of velocity profiles with η for various values of a .

Fig.4: Represents the dimensionless parameter X with horizontal velocity profile. From this figure, it is noticed that the value of X increases with decreases in the velocity profile. here the flow is adjacent to a stretching sheet.

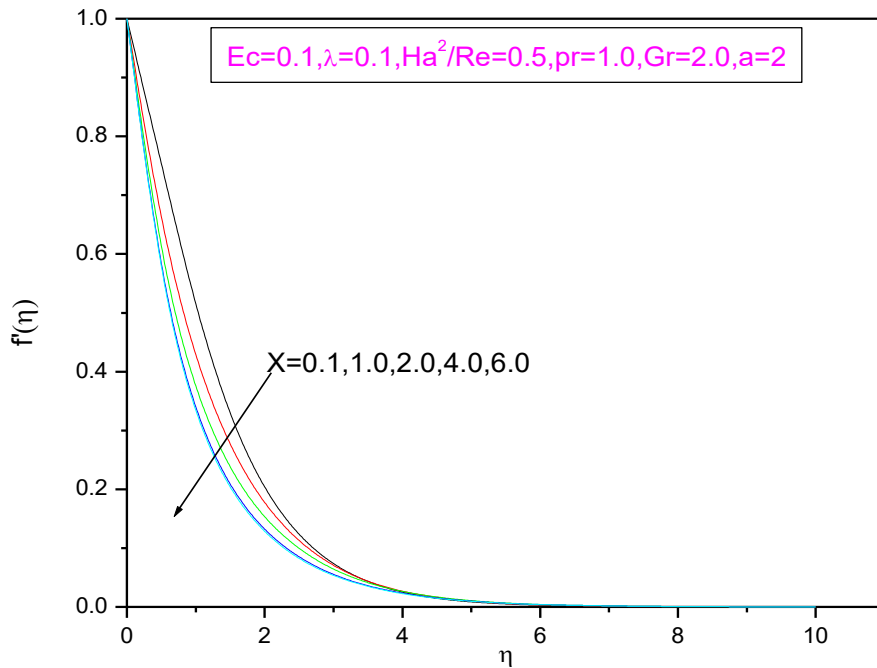


Fig.4. Variations of velocity profiles with η for different values of X.

Fig.5: It is observed from this figure that temperature decreases with increase in the values of a. Further, it is noticed that the thermal boundary layer thickness increases with increase in the value of a. for positive value of a, heat transfer decreases. which indicates that, the flow of heat transfer is directed from the wall to the ambient fluid whereas the rate of heat transfer in the boundary layer increases near the wall.

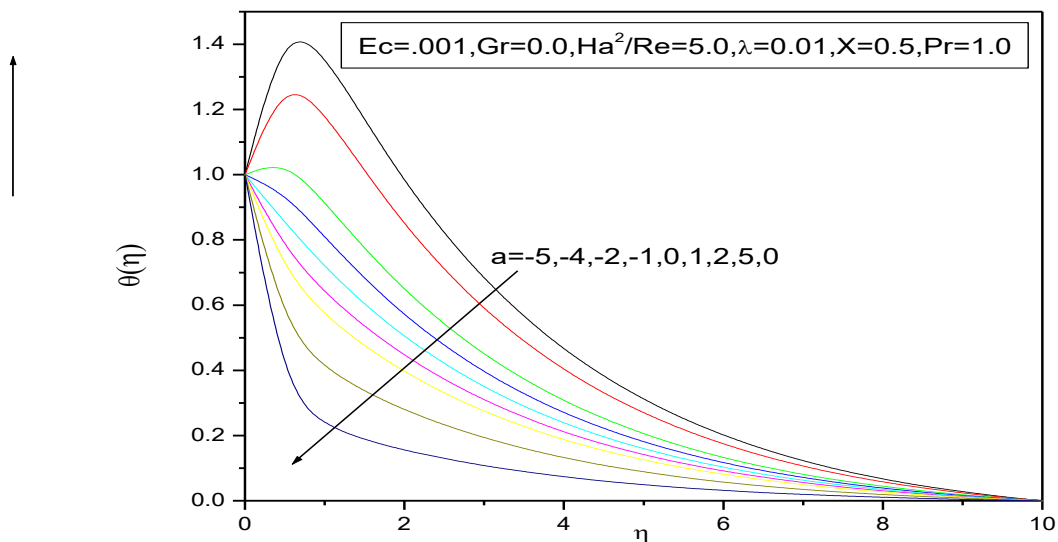


Fig.5. Temperature profiles vs. η for various values of a.

Fig.6: depicts the temperature profile in the fluid for various values of $\frac{Ha^2}{Re}$, for $a = -2$ and $Gr = 0, 0.5$. It is

noticed that an increase in the strength of magnetic field i.e Lorentz force leads to an increase in the temperature far away from the wall, within the thermal boundary layer but the effect of magnetic field near the wall is to decrease the temperature in the absence of Grashof Number. When the magnetic field increases, the thermal boundary layer thickness increases.

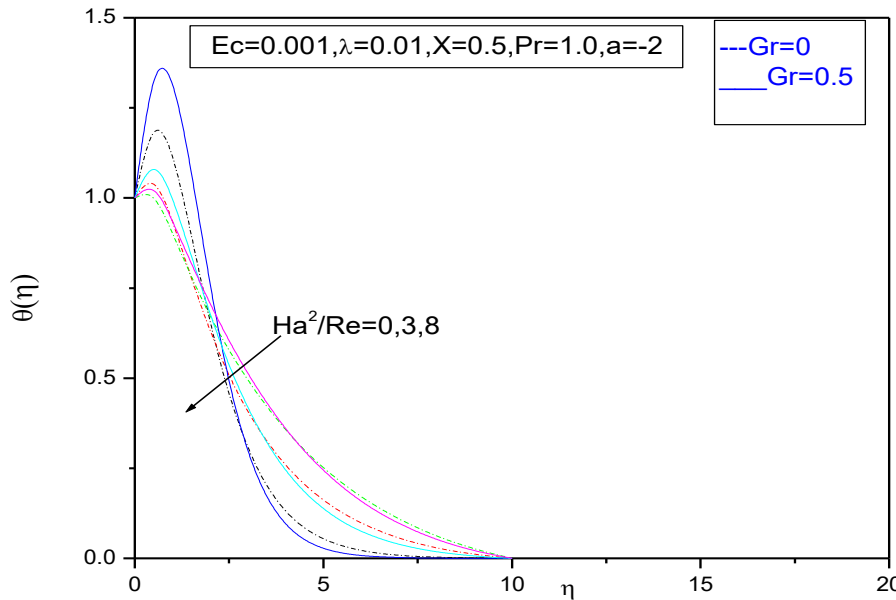


Fig.6. Temperature profiles vs. η for various values of Ha^2/Re and Gr .

Fig7: and it is noticed that increase in Grashof number, increase in temperature up to certain value of η and suddenly decreases and decays asymptotically to zero. Further it is observed that this increase in temperature is due to the temperature difference between stretched wall and the surrounding fluid. When Grashof number leads to increases, the thermal boundary layer thickness decreases.

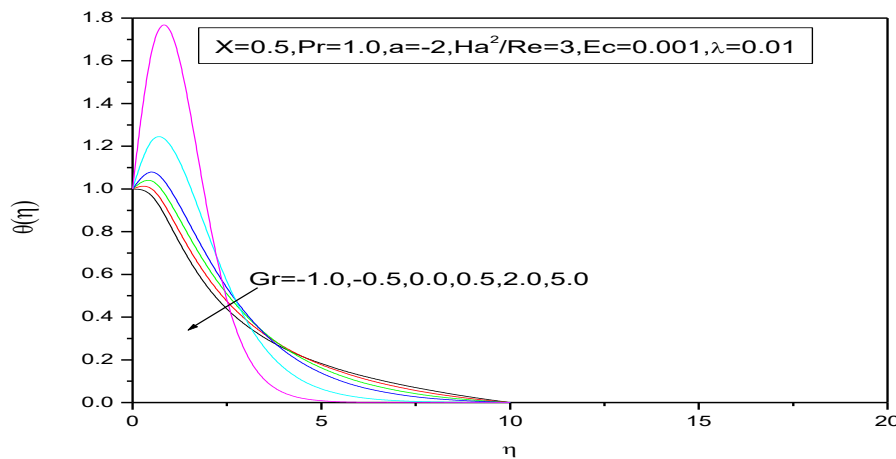


Fig7 temperature profile for various values of Gr

Fig.8: Represents the temperature profile $\theta(\eta)$ for various values of X along η for different values of $a = -1, -2$ and also Grashoff number $Gr = 1.0$. It is noticed that the effect of increasing X on $\theta(\eta)$ is more effective for $a = -2$ than compared to the results obtained in the case when $a = -1$. It is interesting to note the behaviour of X on $\theta(\eta)$, is that the temperature overshoots near the wall for small value of X , for $a = -2$, whereas the overshoot diminishes when a is enhanced to -1 for all other values of X . It is also observed that the boundary layer thickness decreases with an increase in X .

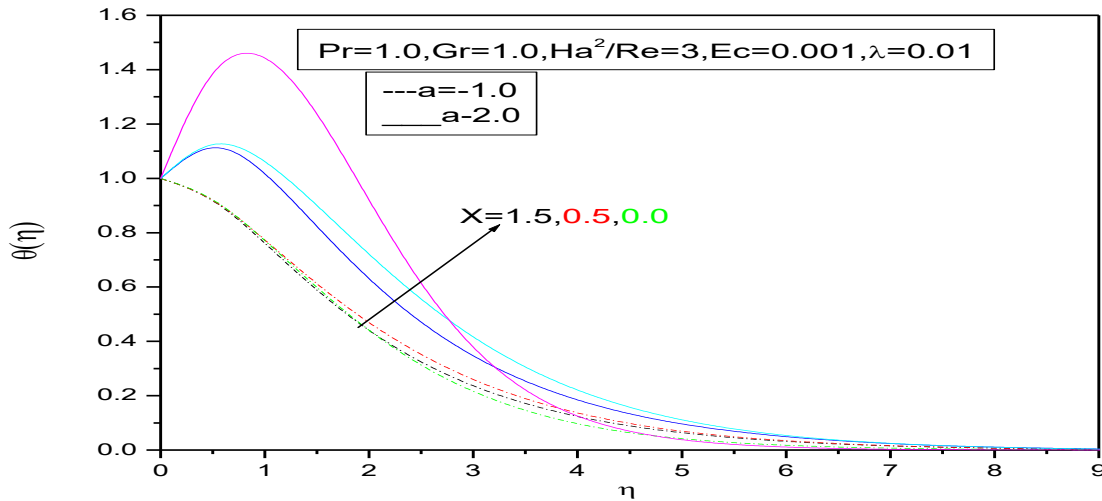


Fig.8. Temperature profiles vs. η for various values of a and X .

Fig.9: Represents the variation of temperature profiles $\theta(\eta)$ for various values of magnetic field parameter ($Ha^2/Re = 0, 6, 8$) for two values of X . When X increases, temperature decreases, all other fixed values of other involved parameters except when the value of parameter $a = 5$. It is also to be noticed that thermal boundary layer thickness increases as X decreases and the effect of magnetic field is to increase the temperature for both values of X . This is due to the Lorentz force the temperature increases.

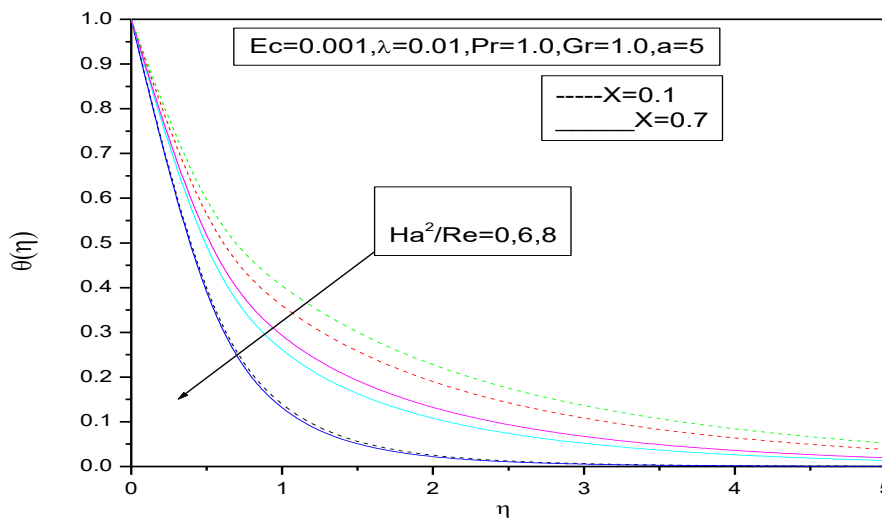


Fig.9. Temperature profiles vs. η for various values of Ha^2/Re and X when $a=5$.

Fig.10: Represents the effect of Prandtl number Pr on dimensionless heat transfer parameter θ . It is noticed from this figure that as Prandtl number Pr increases temperature profile decreases. When Prandtl number Pr is small, heat diffuses quickly compared to the velocity (momentum), especially for liquid metals, (low Prandtl number) the thickness of the thermal boundary layer is much bigger than the momentum boundary layer. Fluids with lower Prandtl number have higher thermal conductivities where. Hence the rate of cooling in conducting flows increases due to the Prandtl number.

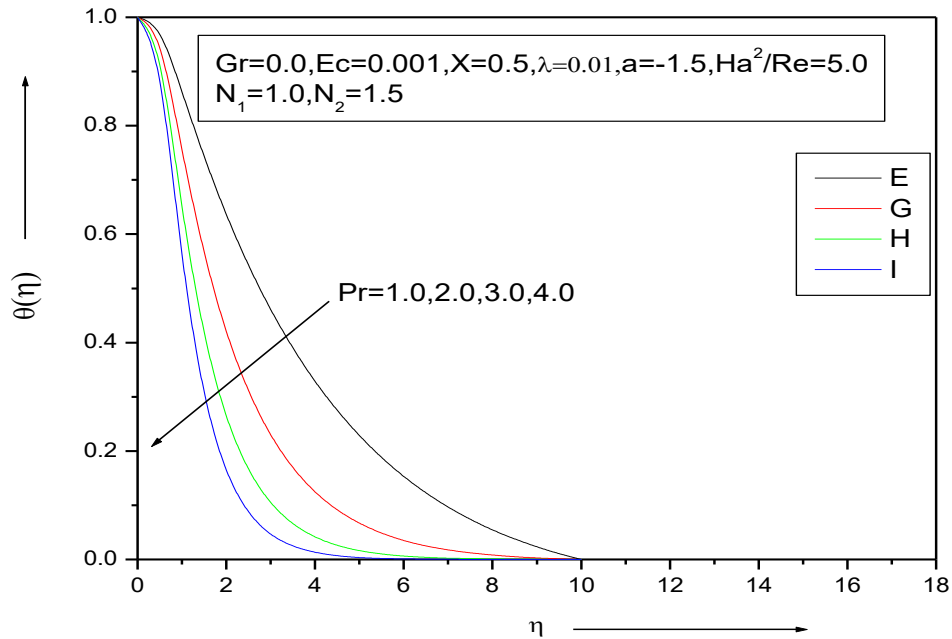


Fig10.Variation of temperature with η for different values of Pr

Fig .11: Represents the effect of porous parameter $N1$ over velocity profile. Porous parameter increases, velocity decreases. Due to this, the velocity decreases in the boundary layer.

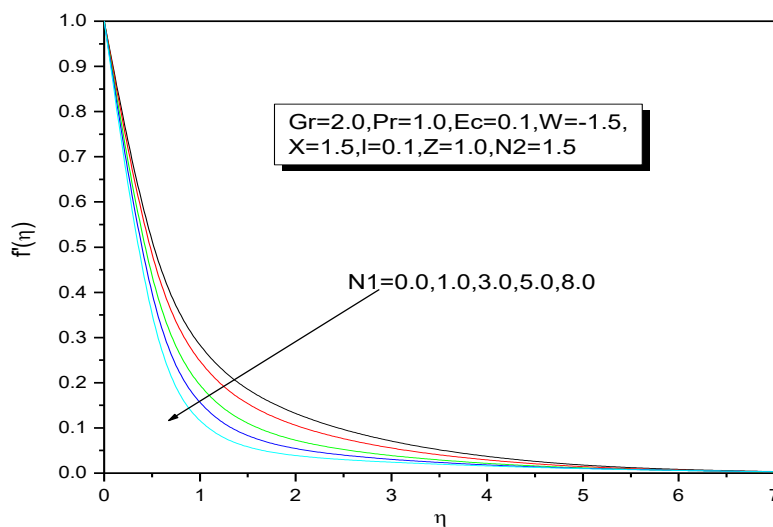


Fig.11.Temperature profile vs. η for various values of $N1$

Fig.12: Represents the effect of inertia coefficient N_2 in the velocity profile. From this we conclude that due to the N_2 , the thickness of momentum of boundary layer decreases.

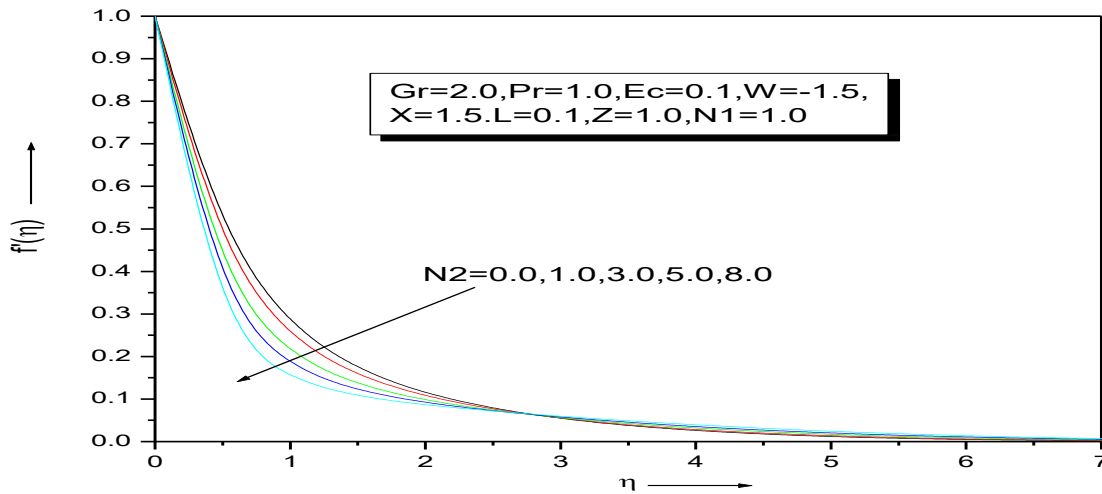


Fig.12. Temperature profile vs. η various values of N_2 .

Fig.13 depicts the effect of heat source/sink parameter λ . It is observed that the boundary layer generates, the energy, which causes the temperature profiles to increase with increasing the values of $\lambda > 0$ (heat source) whereas in the case of $\lambda < 0$ (absorbtion) boundary layer absorbs energy resulting in the temperature to fall considerably with decreasing in the value of $\lambda < 0$.

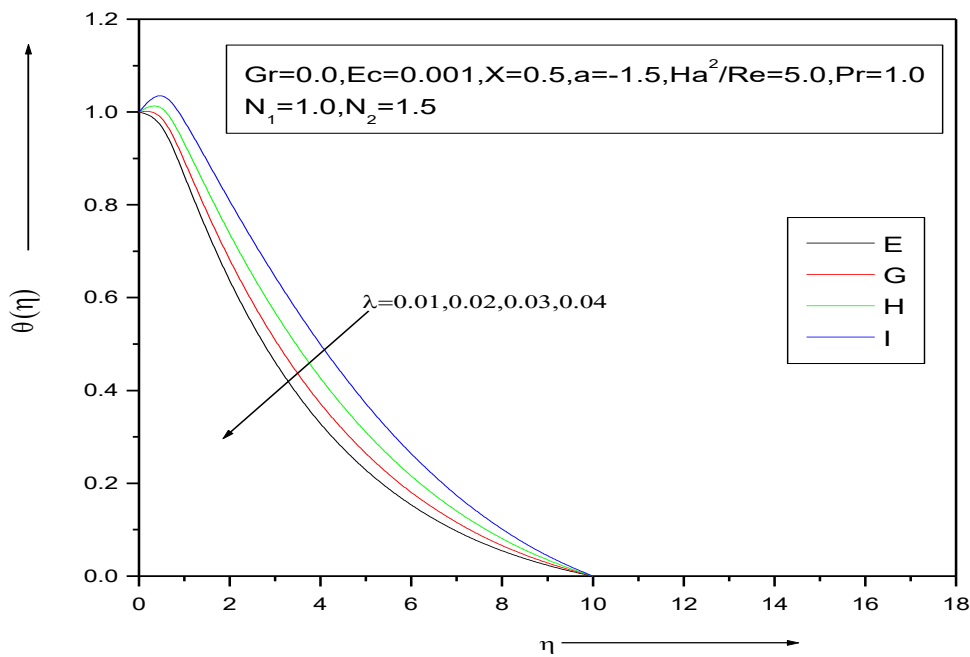


Fig13 Variation of temperature with η for different values of λ

Fig14:depicts dimensionless temperature field for various values of K,with fixed values of other involved parameters.It is observed from the figure that ,K increases,the temperature profiles and the thermal boundary layer thickness also increase.

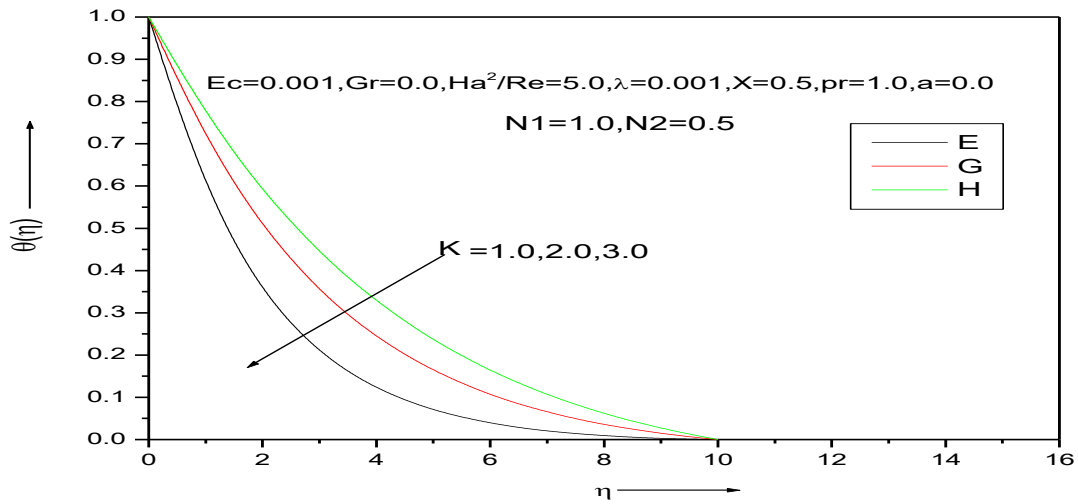


Fig14:Effects of K on the temperature profiles $\theta(\eta)$,Where $K = \frac{4\sigma^* T_\infty^3}{k^* k}$ Radiation Parameter.

Fig15:Effect of porous para meter N1 on a temperature profiles and it is noticed that ,temperature increases with the increase of porous parameter,which offers resistance to the flow resulting in the increase of temperature in the boundary layer.

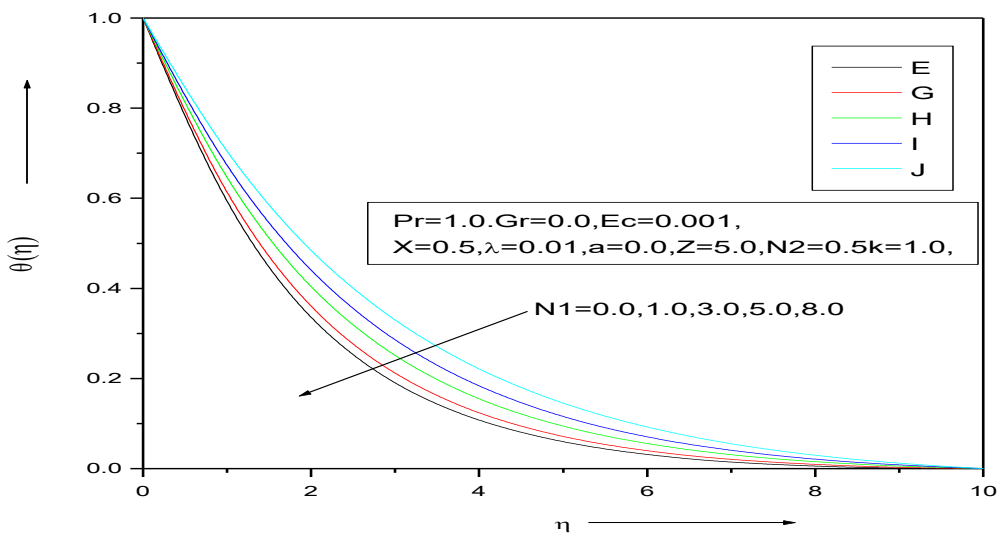


Fig 15: Effect of N1 on the temperature profiles $\theta(\eta)$

Fig16:Effect of drag coefficient of porous medium N_2 .From the figure it is noticed that the effect of drag coefficient is to increase the temperature profile in the boundary layer.Which implies boundary layer thickness also increases.

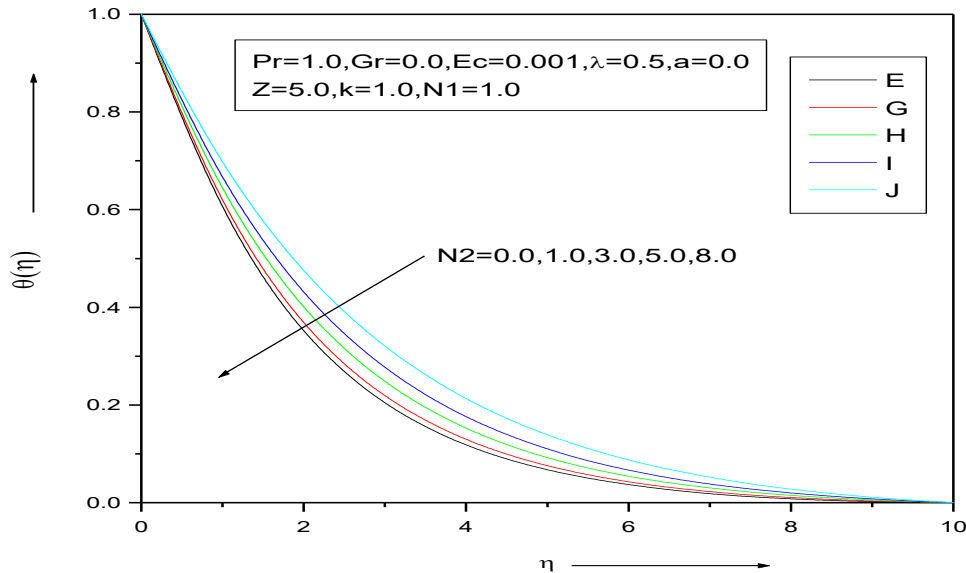


Fig 16: Effect of N_2 on the temperature profiles $\theta(\eta)$

References

1. Gad-el-Hak, M: The fluid mechanics of microdevices-The Freeman scholar lecture. ASME. J. Fluids. Engng 121, 5-33 (1999)
2. T. Hayat, T. Javed, Z. Abbas: Slip flow and heat transfer of a second grade fluid past a stretching sheet through a porous space. Int Journal of Heat and Mass transfer 51 (2008) 4528-4534.
3. Bikash Sahoo: Flow and heat transfer of a non-Newtonian fluid past a stretching sheet with partial slip, Commun Non linear Sci Numer Simulat 15 (2010).
4. Rao I. J., Rajgopal KR: The effect of slip boundary condition on the flow of fluids in a channel. Acta 1999, 135: 113-26.
5. E. M. A. Elbasha, Heat transfer over and exponentially stretching continuous surface with suction. Arch. Mech 53 (2001) 643-651.
6. P. Donald Ariel: Axisymmetric flow due to a stretching sheet with partial slip Int Journal computers and mathematics with Application 54 (2007) 1169-1183.
7. Bikash Sahoo, Younghae Do: Effects of slip on sheet driven flow and heat transfer of a third grade fluid past a stretching sheet. Int. Communications in Heat and Mass Transfer 37 (2010) 1064-1071.

*corresponding Author email: msabel2001@yahoo.co.uk